Title: "Manganese binding to Rubisco could drive a photorespiratory pathway that increases the energy efficiency of photosynthesis."

Authors' Names and Affiliations: Arnold J. Bloom, Department of Plant Sciences, University of California at Davis, Davis, CA 95616; Kyle M. Lancaster, Department of Chemistry and Chemical Biology, Cornell University, Ithaca, NY 14853.

Corresponding Author: Arnold J. Bloom ajbloom@ucdavis.edu

Abstract

Most plants, contrary to popular belief, do not waste over 30% of their photosynthate in a futile cycle called photorespiration. Rather, the photorespiratory pathway generates additional malate in the chloroplast that empowers many energy-intensive chemical reactions such as those involved in nitrate assimilation. The balance between carbon fixation and photorespiration, thus, determines plant carbon/nitrogen balance and protein concentrations. Plant protein concentrations, in turn, depend not only on the relative concentrations of carbon dioxide and oxygen in the chloroplast, but on the relative activities of magnesium and manganese, metals that associate with several key enzymes in the photorespiratory pathway and alter their function. Understanding the regulation of these processes is critical for sustaining food quality under rising CO_2 atmospheres.

Introduction

Rubisco, the most prevalent protein on the planet [1], suffers from a split personality: it catalyzes both a carboxylation reaction that initiates the C_3 carbon fixation pathway and an oxidation reaction that initiates the photorespiratory pathway (**Fig. 1**). The C_3 carbon fixation pathway expends 18 ATP and 12 NADPH per molecule of fructose-6-phosphate generated and 6 RuBP regenerated. The photorespiratory pathway allegedly expends 3.5 ATP and 2 NADPH per RuBP oxygenated and regenerated, but does not result in any net production of sugar [2]. Therefore, photorespiration is generally considered to be a futile cycle [3,4], a vestige of the high CO_2 and low O_2 atmospheres that existed when plants first evolved [5]. Yet the oxidation reaction of photorespiration has persisted for eons across all known forms of Rubisco [6].

Rubisco contains a metal-binding site [7]. The stoichiometry of CO_2 trapping [8] and ^{31}P and ^{13}C NMR measurements [9] indicate that Mn^{2+} and Mg^{2+} share this binding site, but nearly every *in vitro* study of Rubisco biochemistry during the past four decades has been conducted with only Mg^{2+} present. The RCSB Protein Data Bank includes 10 structures of Rubisco with Mg^{2+} as a ligand, but none with Mn^{2+}. One recent review entitled *Biogenesis and Metabolic Maintenance of Rubisco*, which focuses on the "the structure and function of factors [that bind to] Rubisco," does not mention Mn^{2+} [10]. Another recent review entitled *The Mechanism of Rubisco-Catalysed Oxygenation* contains extensive detail about the mechanism of oxygenation when Mg^{2+} is present, but refers to Mn^{2+} only in the disclaimer "it is likely that the mechanism with Mn^{2+} is different" [11].

This article examines the evidence that Rubisco, malic enzyme, and phosphoglycolate phosphatase—the three enzymes in the chloroplast that catalyze the initial reactions of photorespiration—behave differently when associated with Mn^{2+} rather than with Mg^{2+}. These enzymes when associated with Mn^{2+} may directly produce malate that, in turn, empowers many metabolic pathways including nitrate assimilation. Thus, the photorespiratory pathway may be more energy efficient than previously assumed.

Rubisco

Rubisco has three types [10].

- Most common is Form I Rubisco, found in bacteria and in the stroma of chloroplasts in eukaryotes. It is a hexadecamer containing eight identical large subunits (~55,000 M_r), each with a metal-binding site, and eight small subunits (~15,000 M_r). The large subunits are coded by a single plastomic gene, whereas the small subunits are coded by a nuclear multigene family that consists of 2 to 22 members, depending on species [12]. Complex cellular machinery is required to assemble this form

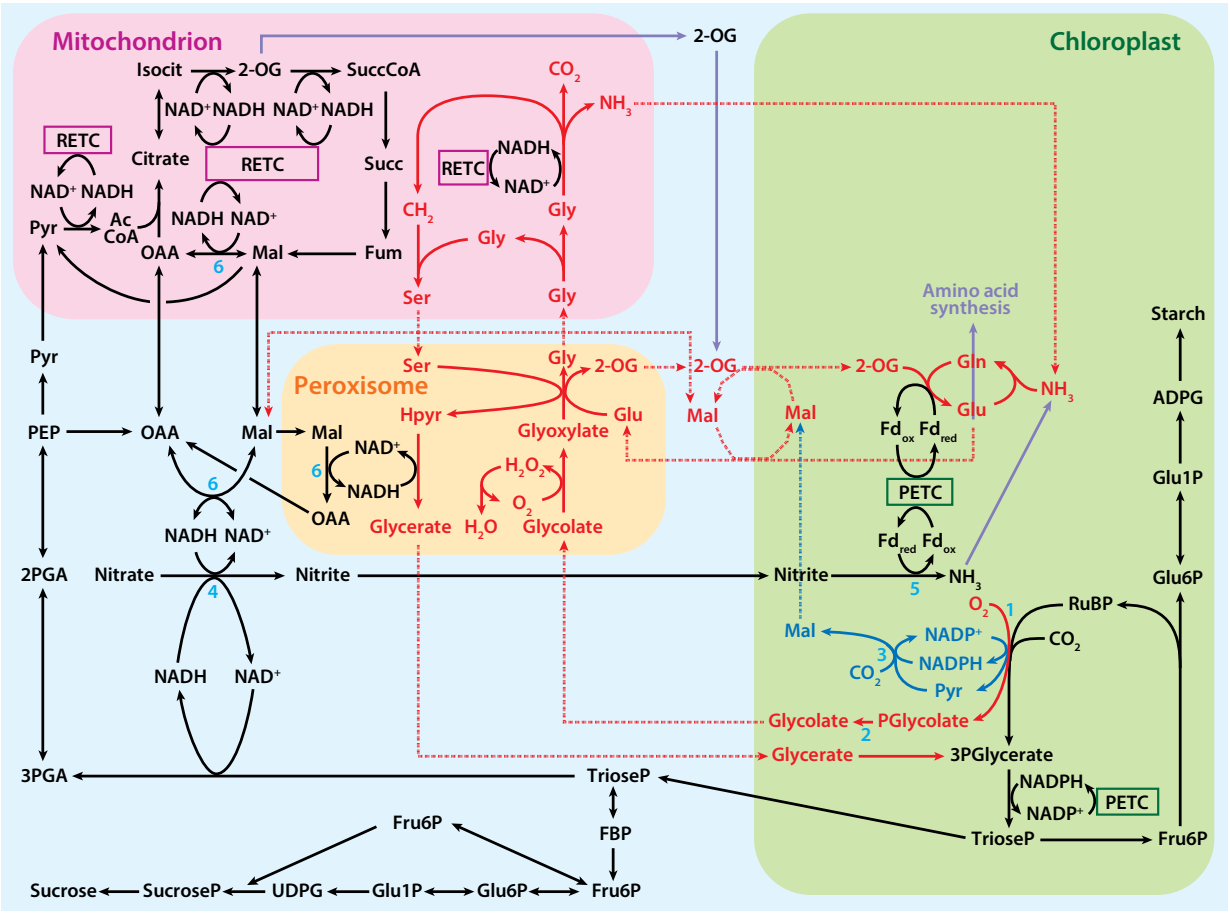

Fig. 1 The proposed photorespiratory pathway within the context of photosynthetic carbon and nitrogen metabolism. The solid red lines represent reactions of the photorespiratory pathway, the solid blue lines represent reactions of the proposed alternative photorespiratory pathway, the solid purple lines represent reactions of amino acid synthesis, and the dotted lines represent associated transport processes. Numbered reactions are catalyzed by the following enzymes: 1. Rubisco, 2. Phosphoglycolate phosphatase, 3. Malic enzyme, 4. Nitrate reductase, 5. Nitrite reductase, and 6. Malate dehydrogenase. PETC designates photosynthetic electron transport chain and RETC, respiratory electron transport chain. [2]

of Rubisco and to maintain its activity [10]. Until this year, Form I Rubisco has resisted all efforts to generate a functional holoenzyme *in vitro* or upon recombinant expression in *E. coli* [13].

- Form II Rubisco, found in bacteria and some dinoflagellates, contains one or more isodimers with subunits that share about 30% identity to the large subunit of Form I Rubisco.
- Form III Rubisco, found in archaea, has one or five isodimers composed of subunits homologous to the large subunit of Form I Rubisco.

Form II and Form III Rubisco show greater similarity in their primary sequence to one another than either do to the large subunit of Form I Rubisco.

The three forms become activated when a specific lysine residue becomes carbamylated, and binds Mn^{2+} or Mg^{2+} [8,9]. NADPH complexes strongly with Rubisco and acts as an effector molecule to maintain the Rubisco catalytic pocket in an open confirmation that more rapidly facilitates CO_2-Mg^{2+} activation when CO_2 and Mg^{2+} are present in suboptimal concentrations [14-17]. The crystal structure of Rubisco with both Mg^{2+} and NADPH as ligands indicates that NADPH binds to the catalytic site of Rubisco through metal-coordinated water molecules [16]. The activated enzyme catalyzes either carboxylation or oxygenation of the enediol form of the five-carbon sugar ribulose-1,5-bisphosphate (RuBP) [7].

The balance between the carboxylation and oxygenation reactions depends on several factors. One factor is the relative amounts of CO_2 and O_2 entering the active site of Rubisco. A second factor is the specificity of the Rubisco for each gas. Under current atmospheres (0.04% CO_2 and 20.94% O_2), Rubisco catalyzes about two to three cycles of C_3 carbon fixation for every cycle of photorespiration [18]. A third factor—one that is usually ignored—is the extent to which Rubisco binds either Mn^{2+} or Mg^{2+}. When Rubisco binds Mn^{2+}, carboxylation and oxidation proceed at similar rates [19], the oxygenation produces singlet oxygen [20,21], and the Mn^{2+} transfers an electron with every oxidation [21]. When Rubisco binds Mg^{2+}, carboxylation accelerates and proceeds four times faster than oxidation [19], but no electrons are transferred [18].

Oxygenation of RuBP via Form I Rubisco bound to Mn^{2+} results in a reaction enthalpy change ($\Delta_r H'$) of –319 kJ mol^{-1} [22]. For comparison, RuBP carboxylation via Form I Rubisco bound to Mg^{2+} has a $\Delta_r H'$ of –21 kJ mol^{-1} [22] and $NADP^+$ reduction to NADPH has a $\Delta_r H'$ of –29 kJ mol^{-1} [23]. The prevailing view is that the –319 kJ mol^{-1} released during RuBP oxidation is dissipated as waste heat [22].

We recently quantified Mn^{2+} and Mg^{2+} activities in isolated tobacco chloroplasts [19]. Activity of an ion is its "effective concentration" in a solution containing a mixture of compounds: chemical potential of the ion depends on its activity in a real solution in the same way that it would depend on concentration in an ideal solution. We assessed Mg^{2+} activity via the increase in fluorescence when the dye mag-fura-2 binds Mg^{2+} (dissociation constant, K_d = 1.5 mM [25]) and Mn^{2+} activity via quenching of this fluorescence when the dye binds Mn^{2+} (K_d = 0.89 μM [26]). The fluorescence without Mn^{2+} quenching was assessed by adding TPEN, a membrane-permeable, non-fluorescent chelator that has K_d's of 5.4×10^{-11} M for Mn^{2+} and 2.0×10^{-2}M for Mg^{2+} [27].

In tobacco chloroplasts, Mn^{2+} was less active than Mg^{2+} (**Fig. 2 a, b**). Increasing the Mn^{2+} activity in the medium by 10-fold increased the chloroplast Mn^{2+} activity by roughly 3-fold (**Fig. 2b**), whereas increasing the Mg^{2+} activity in the medium by 10-fold increased the chloroplast Mg^{2+} activity by roughly 10-fold (**Fig. 2a**). This suggests that regulation of Mn^{2+} and Mg^{2+} activities in chloroplasts, if such exists, occurs primarily at the cellular level.

We also assessed via isothermal titration calorimetry the thermodynamics of metal binding to Form I Rubisco purified from tobacco or to recombinant Form II Rubisco enzyme prepared in *E. coli* based on the sequence from the bacterium *Rhodospirillum rubrum* [19]. The Rubisco purified from tobacco had a lower dissociation constant (K_d) for Mn^{2+} than Mg^{2+} (**Fig. 2d, f**), and so the K_d's of tobacco Rubisco for each metal was similar in magnitude to the activity of each in the chloroplast (**Fig. 2d, f**). Thus, Rubisco in tobacco associated almost equally with both metals and rapidly exchanged one metal for the other.

The thermodynamics of Mn^{2+} binding differed greatly between the Rubiscos from tobacco and a bacterium, whereas the thermodynamics of Mg^{2+} binding was similar for the Rubiscos from these species (**Fig. 2c-f**). Moreover, the ratio of Mn^{2+} contents to Mg^{2+} contents in wheat leaves increased as atmospheric CO_2 increased and when wheat plants received NO_3^- rather than NH_4^+ as a nitrogen source [19]. These results suggest that Rubisco has evolved to improve the energy transfers between photorespiration and NO_3^- assimilation and that plants regulate Mn^{2+} and Mg^{2+} activities in chloroplasts to mitigate detrimental changes in their nitrogen/carbon balance as atmospheric CO_2 varies [19].

Nitrogen

Nitrogen (N) is the element other than carbon, hydrogen, and oxygen that organisms must acquire in greatest amounts from their surroundings [28]. Most organisms can use either NO_3^-, NH_4^+, or organic N compounds as N sources. NH_4^+, however, has the major disadvantage that it becomes toxic when it accumulates in cells because it dissipates the proton concentration gradients across membranes that are vital to electron transport chains and active nutrient transport. To avoid this toxicity, organisms quickly convert the NH_4^+ that they absorb from their surroundings into organic N compounds.

Organisms can accumulate NO_3^- in their tissues to much higher levels than NH_4^+ without toxic effect. In fact, NO_3^- may serve as a metabolically benign osmoticant that, together with monovalent cations such as potassium or sodium, maintains a favorable cellular water balance [28]. The major disadvantage of NO_3^- as an N source is that assimilating it into organic N requires the conversion of the N atom in NO_3^- (oxidation

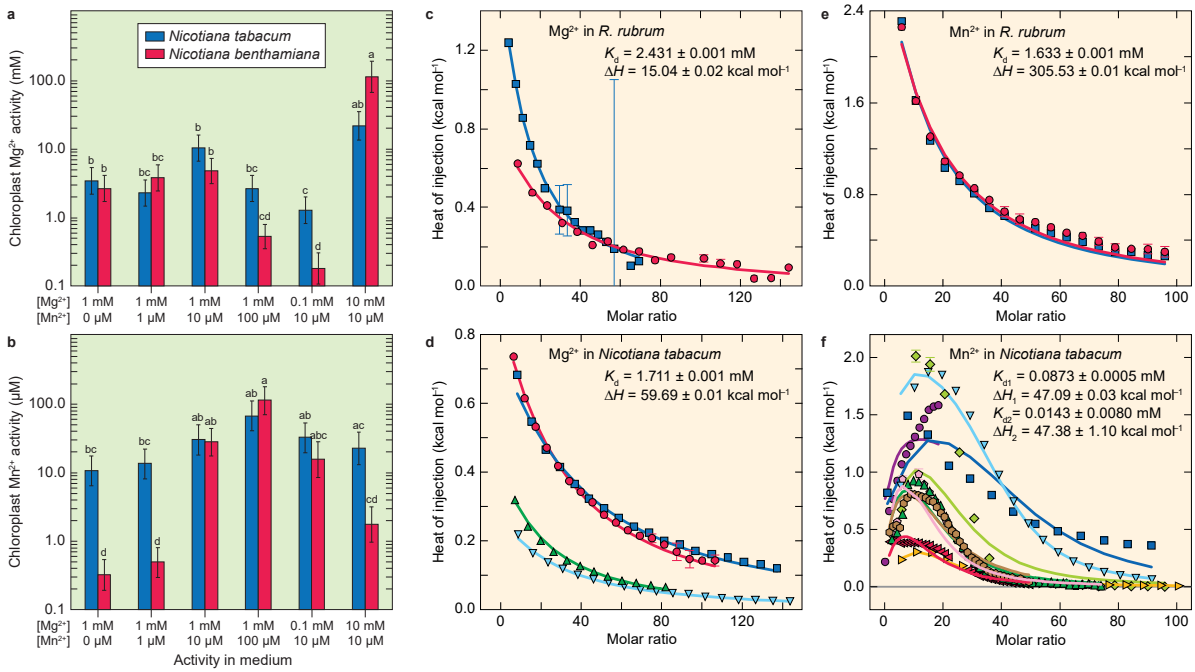

Fig. 2 **a, b**, Mg^{2+} and Mn^{2+} activities in chloroplasts isolated from *Nicotiana tabacum* and *Nicotiana benthamiana* as determined by the ratiometric fluorescent dye mag-fura-2. The chloroplasts were exposed to a buffer containing 330 mM Sorbitol, 20 mM MOPS (pH 7.6) and the designated activities of Mg^{2+} and Mn^{2+}. Shown are least square means and standard errors determined by a mixed linear model (n = 5 – 8). Bars labeled with different letters (a, b, or c) within the panel for a metal were significantly different via a Tukey-Kramer test ($P \leq 0.05$). [19]. **c – f**, Isothermal titration calorimetry measurements of Mg^{2+} or Mn^{2+} binding to Rubisco purified from tobacco *Nicotiana tabacum* or recombinant enzyme prepared in *E. coli* with the sequence from the bacterium *Rhodospirillum rubrum*. Lines designate the means for the fit of a global model to the data from individual experiments. Molar ratio is the concentration of the metal divided by the concentration of Rubisco. The model for Fig. **c** – **e** is a single-site heterogeneous association model (A + B ↔ AB), whereas the model for Fig. **f** is a two-equivalent site heterogeneous association model (A + B + B ↔ AB + B ↔ ABB) with entropy-driven positive cooperativity. Listed are the dissociation constants (K_d) and molar enthalpies (ΔH) estimated from the models with the error limits derived from a Monte Carlo method [24]. Different symbols and colors designate individual experiments conducted under different metal concentrations, Rubisco concentrations, number of injections, injection volumes, times between injections, or strength of temperature feedback control. Error bars for each data point of the isotherm derive from peak-shape analysis (small errors are incorporated into the symbols). [19]

state = +5) into an N atom in an amino acid (oxidation state = –3). This transfer of 8 electrons involves some of the most energy-intensive chemical reactions in life, reactions that together expend the equivalent of 12 ATP per NO_3^- converted into glutamine. For comparison, assimilation of NH_4^+ into glutamine requires the equivalent of only 2 ATP [29]. Thus, microorganisms most prefer organic N forms as N sources and then more strongly prefer the higher energy inorganic N form NH_4^+ over NO_3^-. Accordingly, most phytoplankton [30], fungi [31], cyanobacteria [32], and bacteria [33] absorb and assimilate NO_3^- only in the absence of organic N or NH_4^+.

Plants tend to use NO_3^-, NH_4^+, and organic N as N sources in proportion to their relative availability in the soil solution [28,34], but plants usually cannot compete successfully with soil microorganisms for organic N [35-37]. Also, plants are less successful in competing for soil NH_4^+ because NH_4^+ adsorbs onto the cation exchange complex of most soils and because soil microorganisms use NH_4^+ not only as an N source, but as an energy source via nitrification (microbial conversion of NH_4^+ into NO_3^-). Microorganisms in soils convert nearly all of the applied urea and ammonium fertilizer into NO_3^- within days [38]. Therefore, somewhat by default, NO_3^- serves as the major N source for most plants [28].

Plants depend on NO_3^- even in locations where soil NO_3^- concentrations are low. For instance, many flood-tolerant plants, growing in wetland soils subject to NO_3^- leaching and denitrification (microbial conversion of NO_3^- to N_2), develop aerenchyma that supply the rhizosphere with oxygen and promote nitrification on root surfaces. The NO_3^- thus generated is immediately absorbed by the root [28]. Also, forest soils in which NH_4^+ is the major N source have high rates of gross nitrification that indicate a small but ecologically important NO_3^- pool [39]. Finally, plants that can conduct symbiotic N-fixation are more prevalent in soils deficient in N, but these plants cease N-fixation whenever NO_3^- becomes available in the rhizosphere [40].

This dependence of plants on NO_3^- as an N source persists despite the disproportionately high energy requirements for assimilating NO_3^- into organic N compounds. For some perspective, organic N compounds constitute less than 2% of plant dry mass, but plants expend about 25% of their total energy in shoots [41] and roots [42] on NO_3^- assimilation, both day [43] and night [44]. C_3 plants, when carbon fixation is CO_2-limited, supply this energy without diverting energy from other processes via a pathway that other organisms lack: this pathway is photorespiration [18].

Photorespiration & NO_3^- Assimilation

Multiple lines of evidence link shoot NO_3^- assimilation in C_3 plants to photorespiration [18]. (*a*) Conditions that decrease photorespiration—namely, elevated CO_2 and low O_2—decrease shoot NO_3^- reduction (**Fig. 3**). (*b*) The reduction of the Mn^{2+}-RuBP complex during photorespiration increases the redox potential of the chloroplast [18], which thus stimulates the production of malate [45,46] and promotes its export from chloroplasts [47-49]. Once in the cytoplasm, this malate generates NADH [48] that powers the first step of NO_3^- assimilation, the reduction of NO_3^- to NO_2^- [28]. (*c*) Mutants that alter malate transport or metabolism influence both photorespiration and NO_3^- assimilation [46,50,51].

The rising atmospheric CO_2 concentrations that are anticipated during the next few decades will inhibit photorespiration and initially enhance photosynthesis and primary productivity (**Fig. 4a**). Slower photorespiration, however, will decrease shoot NO_3^- assimilation and eventually decrease plant protein concentrations [44,52,53] (**Fig. 4b**). As plants become protein limited, primary productivity will abate (**Fig. 4a**). This decline in productivity and protein yield pose a major threat to world food security [28].

A meta-analysis of over 7700 observations in 130 plant species found that exposure to elevated CO_2 decreased the foliar concentrations of 25 mineral nutrients by an average of 9.2 ± 0.9% [54]. For example, elevated CO_2 decreased foliar concentrations of nitrogen by 15.9 ± 1.9% and magnesium by 11.6 ± 2.1%. This was not simply the effect of diluting the nutrients through enhanced growth because foliar concentrations of carbon increased by a mere 4.9 ± 2.1%. Of the 25 mineral nutrients assessed, manganese was the only one whose foliar concentration did not decline significantly at elevated CO_2 (1.2 ± 3.0%) [54]. This suggests that foliar Mn^{2+} to Mg^{2+} ratio may play a unique role in acclimation to elevated CO_2.

Metallomics

Over one-third of proteins must be associated with a metal to function properly because metals permit bond angles and redox potentials that polypeptides alone cannot achieve [55,56]. Not just any metal will do: the metal bound to a protein strongly affects its conformation and its participation in chemical reactions [57]. Physiological disorders arise when mis-metallation occurs [58].

Central to this discussion is the extent to which proteins discriminate between Mn^{2+} and Mg^{2+}. These divalent cations have similar effective ionic radii and exhibit similar thermodynamic interactions with other elements [59], and so Mn^{2+} and Mg^{2+} substitute for one another in the metal binding site of many proteins. Manganese, however, has up to five unpaired electrons in its outer shell and readily participates in redox reactions, whereas magnesium has a single pair of electrons in its outer shell and does not readily participate in redox reactions. In particular, Rubisco when associated with Mn^{2+} more strongly favors oxygenation of the substrate RuBP, whereas the enzyme when associated with Mg^{2+} more strongly favors carboxylation [18]. Rubisco when associated with either Mn^{2+} or Mg^{2+} can generate pyruvate directly from RuBP [60].

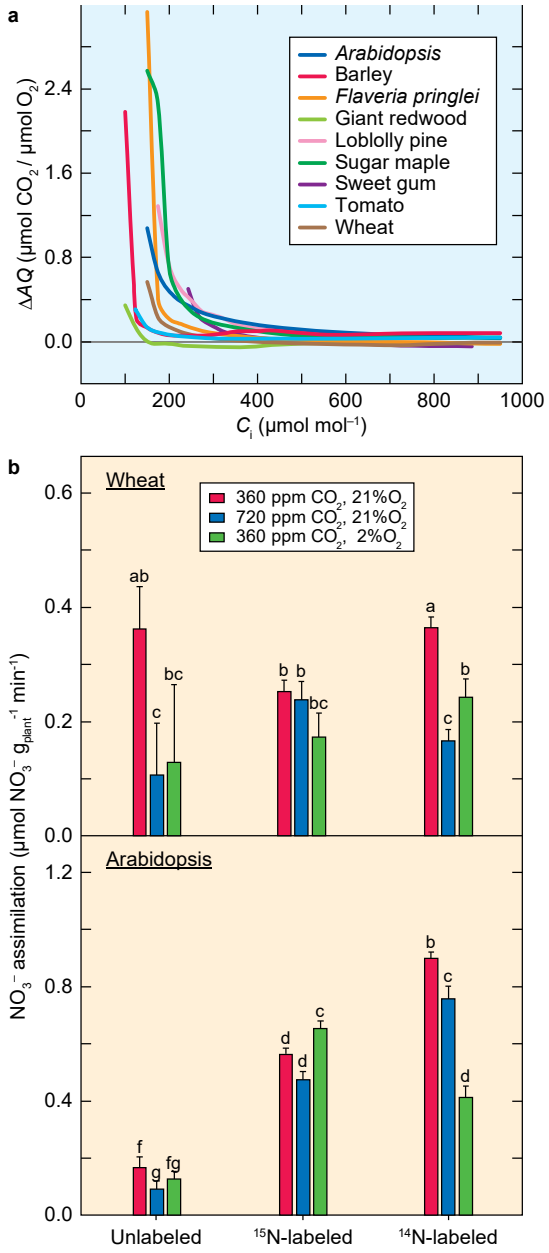

Fig. 3 NO_3^- assimilation. **a**, NO_3^- assimilation vs. leaf internal CO_2 concentration (C_i) in 9 C_3 species. Assimilation was assessed by ΔAQ, the decrease in the ratio of shoot CO_2 consumption to O_2 evolution with a shift from NH_4^+ to NO_3^- nutrition. Note that C_i is substantially less than atmospheric CO_2 concentration because carbon fixation depletes CO_2 and stomata limit CO_2 diffusion. For most C_3 plants, C_i is usually less than 260 μmol mol^{-1} at current atmospheric CO_2 levels of 400 μmol mol^{-1}. At low C_i's, NO_3^- and NO_2^- serve as alternative e^- acceptors to avoid photoinhibition. [18] **b**, Three independent measures of NO_3^- assimilation in spring wheat (cv. Veery) and *Arabidopsis thaliana* cv. Col-0 when exposed to various atmospheres and 0.2 mM NO_3^- nutrition (mean ± SE, n = 6 to 18). For "NO_3^- depletion", decline of NO_3^- concentrations in a nutrient solution indicated plant NO_3^- absorption, and the difference between this absorption and accumulation of free NO_3^- within plant tissues estimated plant NO_3^- assimilation. For "^{15}N-labeled" or "^{14}N-labeled", plants grown on ^{14}N- or ^{15}N-NO_3^- received a pulse of ^{15}N- or ^{14}N-NO_3^-, and the difference between the ^{15}N or ^{14}N enrichment of total N and free NO_3^- estimated plant NO_3^- assimilation. [66]

Malic enzyme has mitochondrial and cytosolic isoforms that primarily catalyze the decarboxylation of malate to pyruvate. The kinetics of this reaction depends on whether the protein is associated with Mn^{2+} or Mg^{2+} [61-63]. By contrast, the plastid isoform of this enzyme in *Arabidopsis* and tobacco primarily catalyzes the so-called reverse reaction (pyruvate + CO_2 + NADPH → malate + $NADP^+$) [64,65]. The influence of Mn^{2+} and Mg^{2+} on this reverse reaction and the affinities for CO_2 or NADPH have not yet been examined.

Phosphoglycolate phosphatase has cytosolic and plastid isoforms that catalyze the hydrolysis of 2-phosphoglycolate to glycolate. This enzyme has a metal binding site that binds either Mn^{2+} or Mg^{2+}, although its affinity for Mn^{2+} is almost seven time stronger than for Mg^{2+} [67]. Nonetheless, most assume that phosphoglycolate phosphatase normally binds Mg^{2+} because its phosphatase activity *in vitro* more than doubles when bound to Mg^{2+} [67,68].

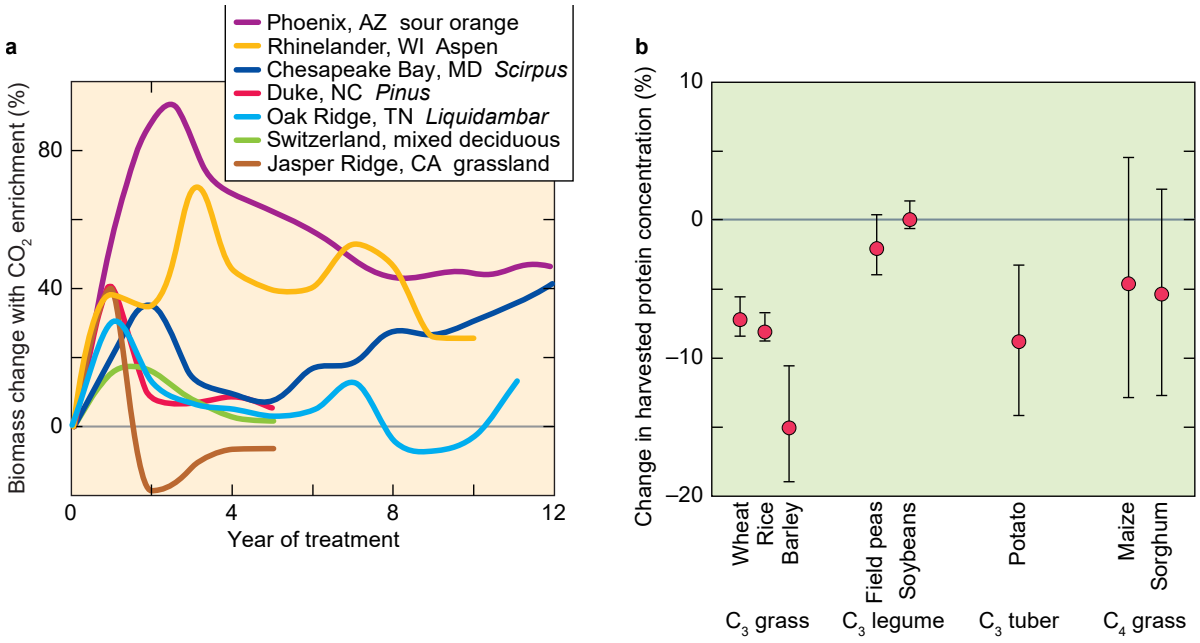

Fig. 4 Plant responses to CO_2 enrichment. **a**, Differences in biomass between elevated (567 µmol mol^{-1}) and ambient (365 µmol mol^{-1}) CO_2 in each year of treatment. Shown are data from seven different studies [69-74] using the designated types of plants. [28] **b**, Percent change in food protein concentration at elevated [CO_2] relative to ambient [CO_2] (mean ± 95% confidence intervals) for crops grown in Free Air CO_2 Enrichment (FACE) experiments. [75]

An Alternative Photorespiratory Pathway?

Changing the Mn^{2+} or Mg^{2+} concentration in the medium produced a proportional change in chloroplast Mn^{2+} or Mg^{2+} activity (**Fig. 2**). The ratio of manganese to magnesium in wheat leaves increased as atmospheric CO_2 increased and when the nitrogen source was NO_3^- instead of NH_4^+ [19]. Therefore, elevated CO_2 and NO_3^- nutrition will probably increase Mn^{2+} activities in chloroplasts relative to Mg^{2+} activities. This will favor photorespiration at the expense of carbon fixation, accelerate shoot NO_3^- assimilation, and restore carbon to nitrogen balance [19].

Mn^{2+} and Mg^{2+} activities in the chloroplast influence the active site conformations and alter the redox reactivities and substrate positioning of Rubisco, malic enzyme, and phosphoglycolate phosphatase and thereby change the kinetics of the reactions that these enzymes catalyze. In the presence of Mg^{2+} alone, the initial reactions of the photorespiratory pathway involving Rubisco and phosphoglycolate phosphatase yield RuBP + O_2 + H_2O → glycolate + 3-phosphoglycerate + P_i in the stroma of the chloroplast [11]:

$C_5H_7O_{11}P_2^{5-} + O_2 + H_2O \rightarrow C_2H_3O_3^- + C_3H_5O_7P^{2-} + HPO_4^{2-}$.

The glycolate translocates to the peroxisome where it, after several reactions in the peroxisome and mitochondrion, is converted to glycerate that translocates back into the chloroplast and regenerates RuBP (**Fig. 1**). The 3-phosphoglycerate (3-PGA) produced during the oxygenation reaction, like that produced during the carboxylation reaction, cycles through triose-phosphate and regenerates RuBP (**Fig. 1**).

By contrast, when plant Rubisco and phosphoglycolate phosphatase are associated with Mn^{2+}, some of the energy being released during RuBP oxidation or hydrolysis of phosphoglycolate may reduce $NADP^+$ to NADPH, and so the initial reaction of photorespiration may become RuBP + $NADP^+$ + H^+ + O_2 + H_2O → pyruvate + glycolate + NADPH + 2P_i (**Fig. 1**):

$C_5H_7O_{11}P_2^{5-} + NADP^+ + H^+ + O_2 + H_2O + 2e^- \rightarrow C_3H_3O_3^- + C_2H_3O_3^- + NADPH + H_2PO_4^- + HPO_4^{2-}$.

When malic enzyme is associated with Mn^{2+}, the second reaction of photorespiration may be pyruvate + CO_2 + NADPH → malate + $NADP^+$ (**Fig. 1**):

$C_3H_3O_3^- + CO_2 + NADPH \rightarrow C_4H_4O_5^{2-} + NADP^+$.

The NADPH required for this reaction may derive from both RuBP oxidation and ferredoxin-$NADP^+$ reduction, but photorespiration becomes more energy efficient if NADPH derives from RuBP oxidation, and so the net reaction may be RuBP + O_2 + CO_2 + H_2O → glycolate + malate + $2P_i$:

$C_5H_7O_{11}P_2^{5-} + O_2 + CO_2 + H_2O + 2e^- \rightarrow C_2H_3O_3^- + C_4H_4O_5^{2-} + 2HPO_4^{2-}$.

Glycolate and malate, which may be generated during the initial reactions of photorespiration, are exported from the chloroplast (**Fig. 1**). The remainder of the photorespiratory pathway proceeds as described in textbooks [2]. Remember that the C:N ratio in plants is roughly 20:1, and so the moles of malate generated via photorespiration need be only about 5% of the moles CO_2 fixed.

Prior studies have not considered the generation of malate from RuBP. Indeed, few experiments have subjected isolated chloroplasts to conditions that promote photorespiration. Lacking entirely are *in vitro* experiments that include all the components of this proposed alternative pathway: Rubisco, malic enzyme, phosphoglycolate phosphatase, RuBP, Mn^{2+}, $NADP^+$, CO_2, and O_2. *Consequently, current evidence for this alternative pathway is purely circumstantial.*

Evidence for an Alternative Pathway

One line of evidence that supports the proposed alternative photorespiratory pathway is the temperature response of C_4 versus C_3 plants. Temperature influences the balance between C_3 carbon fixation and photorespiration in two ways. First, as temperature rises, the solubility of CO_2 in water decreases more than the solubility of O_2, resulting in a lower CO_2:O_2 ratio. Second, the enzymatic properties of Rubisco shift with increasing temperature, stimulating the reaction with O_2 to a greater degree than the one with CO_2. Warmer temperatures, therefore, favor photorespiration over C_3 carbon fixation, and photosynthetic conversion of absorbed light into sugars becomes less efficient [76]. Based on the temperature response of Rubisco carboxylation and oxygenation and on the textbook biochemical pathway for photorespiration, C_4 plants should be more competitive in regions where the mean monthly air temperature exceeds 22°C [77].

In fact, the quantum yield of photosynthesis in an ambient CO_2 and O_2 atmosphere does not differ significantly between C_3 and C_4 species at temperatures between 25° and 30°C [78]. Only under hotter and drier conditions does C_4 carbon fixation become more efficient than C_3 fixation, and C_3 species continue to dominate in most locations worldwide. This is consistent with the contention that C_3 carbon fixation is more efficient than previously thought: if photorespiration follows the alternative pathway proposed here, both C_3 and C_4 carbon fixation at moderate temperatures will expend the equivalent of about 11 ATPs per CO_2 fixed [18].

A second line of evidence supporting an alternative pathway is the apparent similarities among Rubiscos isolated from various sources. Recent studies have assessed the kinetics of carboxylation versus oxygenation for Rubisco isolated from a wide range of species [6,79]. Among 28 terrestrial plant species representing different phylogenetic lineages, environmental adaptations, and photosynthetic mechanisms, Rubisco had affinities for CO_2 and O_2 that varied less than 6% (K_c = 10.5 ± 0.5 μM and K_o = 392 ± 23 μM) when the enzyme was associated with Mg^{2+} [79]. This has led to the belief that "despite slow catalysis and confused substrate specificity, all ribulose bisphosphate carboxylases may be nearly perfectly optimized" [80]. On the contrary, recent results indicate that Rubisco properties vary more widely when the enzyme is associated with Mn^{2+} [19] (**Fig. 2**). This supports the contention that Rubisco when associated with Mn^{2+} has evolved to improve the energy transfers between photorespiration and other metabolic processes [19].

A third line of evidence is that plants increase their rate of photosynthetic CO_2 uptake via the photorespiratory pathway when assimilating NO_3^- into amino acids by fixing carbon to both organic acids and carbohydrates [81]. Modification of the widely-used Farquhar, von Caemmerer, and Berry photosynthesis model to include the carbon and electron requirements for NO_3^- assimilation via the photorespiratory pathway improves predictions of rates for photosynthetic CO_2 uptake and photosynthetic electron transport. Thus, photorespiration improves photosynthetic performance despite reducing the efficiency of Rubisco carboxylation [81].

A fourth line of evidence supporting an alternative pathway is that models of plant CO_2 exchange have assumed that photorespiration evolves one CO_2 for every two oxygenations of RuBP [82,83]. This depends on the supposition that the initial photorespiratory reactions in the chloroplast are RuBP + O_2 + H_2O → glycolate + 3-phosphoglycerate + P_i. The alternative pathway, whereby RuBP + O_2 + CO_2 + H_2O → glycolate + malate + $2P_i$, would evolve less CO_2 per oxygenation and might explain some of the inconsistencies between current models with observations of CO_2 fluxes at higher temperatures [82,83].

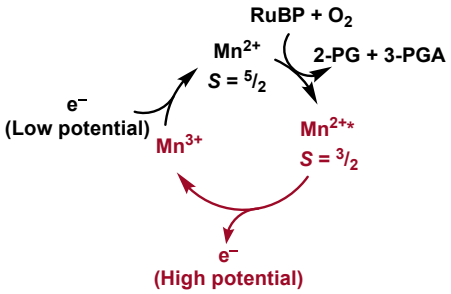

Fig. 5 Treatment of Mn^{2+}-Rubisco with RuBP and O_2 produces a photophysically-active, spin-flipped S = $^3/_2$ Mn^{2+*} excited state. In the red pathway, the excited state transfers a high-potential electron towards reduction of $NADP^+$ to NADPH.

One study has examined Mg and Mn contents in leaves exposed to different temperatures and atmospheric CO_2 concentrations [84]. In Scots pine needles, elevated CO_2 and higher temperatures decreased the ratio of Mg content to Mn content. If leaf content of these metals is related to their activities, then these results are consistent with the observed lower specificity for Rubisco carboxylation at higher temperatures [85].

A fifth line of evidence is that certain grasses and eudicot species, including most C_3–C_4 intermediates, conduct C_2 photosynthesis whereby they transport photorespiratory glycine from the mesophyll to bundle sheath cells for decarboxylation by glycine decarboxylase and re-fix the CO_2 thus released by the Calvin-Benson cycle in the bundle sheath [86,87]. The persistence of substantial Rubisco oxidation even within species having CO_2 concentrating mechanisms indicates that photorespiration is more efficient than previously assumed.

A sixth line of evidence is that an aerated solution of activated Mn^{2+}-Rubisco exhibits a long-lived chemiluminescence when RuBP is added [21]. This chemiluminescence seems to derive from a spin-flip within the Mn^{2+} 3d manifold, leading to an excited quartet ($S = {}^3/_2$) d^5 electronic configuration that decays over the course of 1 to 5 minutes back to the sextet ($S = {}^5/_2$) ground state electronic configuration (**Fig. 5**). Excited states are intrinsically better oxidants and reductants (larger reduction/oxidation potentials) than their corresponding ground states [88-90], thus, the observed chemiluminescence may indicate that the RuBP-O_2-Mn^{2+}-Rubisco excited state is quenched via electron transfer and that the liberated reducing equivalent participates in the reduction of $NADP^+$ to NADPH. In this way, oxidation of RuBP via O_2 may proceed in a spin-allowed manner; meanwhile the Mn^{2+} remains "innocent" in the generation of the oxygenated RuBP precursor. Mn^{2+}-centered redox may still proceed, with oxidation of excited Mn^{2+} to Mn^{3+} occurring in a manner independent of, but parallel to, substrate oxidation. What remains uncertain is how reduction of Mn^{3+} to Mn^{2+} proceeds, although multiple possibilities exist including biological electron transfer from some donor such as reduced plastocyanins, or dissociation of Mn^{3+} and disproportionation to Mn^{2+} and Mn^{4+}.

The last line of evidence is that each of the three enzymes in the initial reactions of the photorespiratory pathway has a metal binding site that binds either Mn^{2+} or Mg^{2+}, but often has a stronger affinity for Mn^{2+}. Is this mere coincidence or do plants regulate these enzymes to optimize synthesis of malate? Malate is a stable organic acid that is readily transported across biological membranes and generates reducing power when and where it is needed through the reaction malate + NAD^+ + $2e^-$ → oxaloacetate + NADH (catalyzed by malate dehydrogenase).

Conclusions

Studies of photosynthesis have suffered under the misconception that the photorespiratory pathway in most plants dissipates over 30% of the photosynthate as waste heat and that this futile cycle has continued through the ages because most plants have reached an evolutionary dead-end. Proposed here is an alternative pathway for photorespiration that is consistent with evolutionary theory: plants have not made a historic error;

rather, photorespiration stimulates the production of malate in chloroplasts and generates reductant for energy-intensive processes such as nitrate assimilation. Photorespiration, thus, allows plants to gain nearly exclusive use of soil nitrate as a nitrogen source, because few other organisms can afford the energy to convert this low-energy nitrogen form into organic forms.

Furthermore, the proposed alternative photorespiratory pathway (**Fig. 1**) may generate additional malate in the chloroplast without diverting photosynthate from growth. Evidence for this pathway, however, is sparse perhaps because experiments conducted during the last four decades have not included all of the required ligands (*i.e.*, Rubisco, malic enzyme, phosphoglycolate phosphatase, RuBP, Mn^{2+}, $NADP^{+}$, CO_2, and O_2). Hence, the next experimental steps are straightforward.

Corresponding Author

Arnold J. Bloom: ajbloom@ucdavis.edu

Acknowledgements

This work was funded by NSF grants IOS-16-55810 and IOS-13-58675, USDA-IWYP-16-06702, and the John B. Orr Endowment. We thank Fred Fox for his comments on the manuscript.

Author contributions.

A.J.B. wrote most of the manuscript and K.M.L. contributed the section on the chemistry of manganese electron transfers and helped edit the entire manuscript.

References Cited

1 Raven, J. A. Rubisco: still the most abundant protein of Earth? *New Phytol.* **198**, 1-3 (2013).

2 Foyer, C. H., Bloom, A. J., Queval, G. & Noctor, G. Photorespiratory metabolism: Genes, mutants, energetics, and redox signaling. *Annu. Rev. Plant Biol.* **60**, 455-484 (2009).

3 Walker, B. J., VanLoocke, A., Bernacchi, C. J. & Ort, D. R. The costs of photorespiration to food production now and in the future. *Annu. Rev. Plant Biol.* **67**, 107-129 (2016).

4 Betti, M. *et al.* Manipulating photorespiration to increase plant productivity: recent advances and perspectives for crop improvement. *J. Exp. Bot.* **67**, 2977-2988, doi:10.1093/jxb/erw076 (2016).

5 Ort, D. R. *et al.* Redesigning photosynthesis to sustainably meet global food and bioenergy demand. *Proc. Nat. Acad. Sci. USA* **112**, 8529-8536, doi:10.1073/pnas.1424031112 (2015).

6 Shih, P. M. *et al.* Biochemical characterization of predicted Precambrian RuBisCO. *Nature Communications* **7**, 10382, doi:10.1038/ncomms10382 (2016).

7 Tabita, F. R., Satagopan, S., Hanson, T. E., Kreel, N. E. & Scott, S. S. Distinct form I, II, III, and IV Rubisco proteins from the three kingdoms of life provide clues about Rubisco evolution and structure/function relationships. *J. Exp. Bot.* **59**, 1515-1524, doi:10.1093/jxb/erm361 (2008).

8 Miziorko, H. M. & Sealy, R. C. Characterization of the ribulosebisphosphate carboxylase-carbon dioxide-divalent cation-carboxypentitol bisphosphate complex. *Biochemistry* **19**, 1167-1171, doi:10.1021/bi00547a020 (1980).

9 Pierce, J. & Reddy, G. S. The sites for catalysis and activation of ribulosebisphosphate carboxylase share a common domain. *Arch. Biochem. Biophys.* **245**, 483-493 (1986).

10 Bracher, A., Whitney, S. M., Hartl, F. U. & Hayer-Hartl, M. Biogenesis and metabolic maintenance of Rubisco. *Annu. Rev. Plant Biol.* **68**, 29-60 (2017).

11 Tcherkez, G. The mechanism of Rubisco-catalysed oxygenation. *Plant Cell Environ.* **39**, 983-997 (2016).

12 Ogawa, S., Suzuki, Y., Yoshizawa, R., Kanno, K. & Makino, A. Effect of individual suppression of RBCS multigene family on Rubisco contents in rice leaves. *Plant Cell Environ.* **35**, 546-553 (2012).

13 Aigner, H. *et al.* Plant RuBisCo assembly in *E. coli* with five chloroplast chaperones including BSD2. *Science* **358**, 1272-1278 (2017).

14 Chollet, R. & Anderson, L. L. Regulation of ribulose 1,5-bisphosphate carboxylase-oxygenase activities by temperature pretreatment and chloroplast metabolites. *Arch. Biochem. Biophys.* **176**, 344-351, doi:http://dx.doi.org/10.1016/0003-9861(76)90173-9 (1976).

15 Chu, D. K. & Bassham, J. A. Activation of ribulose 1,5-diphosphate carboxylase by nicotinamide adenine-dinucleotide phosphate and other chloroplast metabolites. *Plant Physiol.* **54**, 556-559, doi:10.1104/pp.54.4.556 (1974).

16 Matsumura, H. *et al.* Crystal structure of rice Rubisco and implications for activation induced by positive effectors NADPH and 6-phosphogluconate. *Journal of Molecular Biology* **422**, 75-86 (2012).

17 McCurry, S. D., Pierce, J., Tolbert, N. E. & Orme-Johnson, W. H. On the mechanism of effector-mediated activation of ribulose bisphosphate carboxylase/oxygenase. *J. Biol. Chem.* **256**, 6623-6628 (1981).

18 Bloom, A. J. Photorespiration and nitrate assimilation: a major intersection between plant carbon and nitrogen. *Photosynth. Res.* **123**, 117-128, doi:10.1007/s11120-014-0056-y (2015).

19 Bloom, A. J. & Kameritsch, P. Relative association of Rubisco with manganese and magnesium as a regulatory mechanism in plants. *Physiol. Plant.* **161**, 545-559, doi:10.1111/ppl.12616 (2017).

20 Mogel, S. N. & McFadden, B. A. Chemiluminescence of the Mn^{2+}-activated ribulose-1,5-bisphosphate oxygenase reaction - evidence for singlet oxygen production. *Biochemistry* **29**, 8333-8337, doi:10.1021/bi00488a019 (1990).

21 Lilley, R. M. C., Wang, X. Q., Krausz, E. & Andrews, T. J. Complete spectra of the far-red chemiluminescence of the oxygenase reaction of Mn^{2+}-activated ribulose-bisphosphate carboxylase/oxygenase establish excited Mn^{2+} as the source. *J. Biol. Chem.* **278**, 16488-16493 (2003).

22 Frank, J., Kositza, M. J., Vater, J. & Holzwarth, J. F. Microcalorimetric determination of the reaction enthalpy changes associated with the carboxylase and oxygenase reactions catalysed by ribulose 1,5-bisphosphate carboxylase/oxygenase (RUBISCO). *Physical Chemistry Chemical Physics* **2**, 1301-1304 (2000).

23 Alberty, R. A. Calculation of standard transformed Gibbs energies and standard transformed enthalpies of biochemical reactants. *Arch. Biochem. Biophys.* **353**, 116-130 (1998).

24 Brautigam, C. A., Zhao, H., Vargas, C., Keller, S. & Schuck, P. Integration and global analysis of isothermal titration calorimetry data for studying macromolecular interactions. *Nat. Protocols* **11**, 882-894, doi:10.1038/nprot.2016.044 (2016).

25 Günther, T. Concentration, compartmentation and metabolic function of intracellular free Mg^{2+}. *Magnesium research* **19**, 225-236 (2006).

26 Golynskiy, M. V., Gunderson, W. A., Hendrich, M. P. & Cohen, S. M. Metal binding studies and EPR spectroscopy of the manganese transport regulator MntR. *Biochemistry* **45**, 15359-15372 (2006).

27 Arslan, P., Di Virgilio, F., Beltrame, M., Tsien, R. & Pozzan, T. Cytosolic Ca^{2+} homeostasis in Ehrlich and Yoshida carcinomas. A new, membrane-permeant chelator of heavy metals reveals that these ascites tumor cell lines have normal cytosolic free Ca^{2+}. *J. Biol. Chem.* **260**, 2719-2727 (1985).

28 Bloom, A. J. The increasing importance of distinguishing among plant nitrogen sources. *Curr. Opin. Plant Biol.* **25**, 10-16, doi:10.1016/j.pbi.2015.03.002 (2015).

29 Bloom, A. J. in *Plant Physiol.* (eds Lincoln Taiz, Eduardo Zeiger, Ian M. Møller, & Angus Murphy) Ch. 13, 353-376 (Sinauer, 2015).

30 Dortch, Q. The interaction between ammonium and nitrate uptake in phytoplankton. *Mar Ecol-Pr* **61**, 183-201 (1990).

31 Hodge, A., Helgason, T. & Fitter, A. H. Nutritional ecology of arbuscular mycorrhizal fungi. *Fungal Ecology* **3**, 267-273, doi:http://dx.doi.org/10.1016/j.funeco.2010.02.002 (2010).

32 Ohashi, Y. *et al.* Regulation of nitrate assimilation in cyanobacteria. *J. Exp. Bot.* **62**, 1411-1424, doi:10.1093/jxb/erq427 (2011).

33 Luque-Almagro, V. M. *et al.* Bacterial nitrate assimilation: gene distribution and regulation. *Biochemical Society Transactions* **39**, 1838-1843 (2011).

34 Britto, D. T. & Kronzucker, H. J. Ecological significance and complexity of N-source preference in plants. *Ann. Bot.* **112**, 957-963, doi:10.1093/aob/mct157 (2013).

35 Näsholm, T., Kielland, K. & Ganeteg, U. Uptake of organic nitrogen by plants. *New Phytol.* **182**, 31-48, doi:10.1111/j.1469-8137.2008.02751.x (2009).

36 Kuzyakov, Y. & Xu, X. Competition between roots and microorganisms for nitrogen: mechanisms and ecological relevance. *New Phytol.* **198**, 656-669, doi:10.1111/nph.12235 (2013).

37 Jones, D. L., Clode, P. L., Kilburn, M. R., Stockdale, E. A. & Murphy, D. V. Competition between plant and bacterial cells at the microscale regulates the dynamics of nitrogen acquisition in wheat (Triticum aestivum). *New Phytol.* **200**, 796-807, doi:10.1111/nph.12405 (2013).

38 Matson, P. A., Naylor, R. & Ortiz-Monasterio, I. Integration of environmental, agronomic, and economic aspects of fertilizer management. *Science* **280**, 112-115 (1998).

39 Stark, J. M. & Hart, S. C. High rates of nitrification and nitrate turnover in undisturbed coniferous forests. *Nature* **385**, 61-64 (1997).

40 Cabeza, R. *et al.* An RNA sequencing transcriptome analysis reveals novel insights into molecular aspects of the nitrate impact on the nodule activity of *Medicago truncatula*. *Plant Physiol.* **164**, 400-411, doi:10.1104/pp.113.228312 (2014).

41 Bloom, A. J., Caldwell, R. M., Finazzo, J., Warner, R. L. & Weissbart, J. Oxygen and carbon dioxide fluxes from barley shoots depend on nitrate assimilation. *Plant Physiol.* **91**, 352-356 (1989).

42 Bloom, A. J., Sukrapanna, S. S. & Warner, R. L. Root respiration associated with ammonium and nitrate absorption and assimilation by barley. *Plant Physiol.* **99**, 1294-1301 (1992).

43 Cousins, A. B. & Bloom, A. J. Oxygen consumption during leaf nitrate assimilation in a C_3 and C_4 plant: the role of mitochondrial respiration. *Plant Cell Environ.* **27**, 1537-1545 (2004).

44 Rubio-Asensio, J. S., Rachmilevitch, S. & Bloom, A. J. Responses of Arabidopsis and wheat to rising CO_2 depend on nitrogen source and nighttime CO_2 levels. *Plant Physiol.* **168**, 156-163, doi:10.1104/pp.15.00110 (2015).

45 Scheibe, R. Malate valves to balance cellular energy supply. *Physiol. Plant.* **120**, 21-26, doi:10.1111/j.0031-9317.2004.0222.x (2004).

46 Obata, T., Florian, A., Timm, S., Bauwe, H. & Fernie, A. R. On the metabolic interactions of (photo) respiration. *J. Exp. Bot.* **67**, 3003-3014 (2016).

47 Backhausen, J. E. *et al.* Transgenic potato plants with altered expression levels of chloroplast NADP-malate dehydrogenase: interactions between photosynthetic electron transport and malate metabolism in leaves and in isolated intact chloroplasts. *Planta* **207**, 105-114 (1998).

48 Taniguchi, M. & Miyake, H. Redox-shuttling between chloroplast and cytosol: integration of intra-chloroplast and extra-chloroplast metabolism. *Curr. Opin. Plant Biol.* **15**, 252-260, doi:http://dx.doi.org/10.1016/j.pbi.2012.01.014 (2012).

49 Voss, I., Sunil, B., Scheibe, R. & Raghavendra, A. S. Emerging concept for the role of photorespiration as an important part of abiotic stress response. *Plant Biol.* **15**, 713-722, doi:10.1111/j.1438-8677.2012.00710.x (2013).

50 Dutilleul, C. *et al.* Mitochondria-driven changes in leaf NAD status exert a crucial influence on the control of nitrate assimilation and the integration of carbon and nitrogen metabolism. *Plant Physiol.* **139**, 64-78 (2005).

51 Schneidereit, J., Hausler, R. E., Fiene, G., Kaiser, W. M. & Weber, A. P. M. Antisense repression reveals a crucial role of the plastidic 2-oxoglutarate/malate translocator DiT1 at the interface between carbon and nitrogen metabolism. *Plant J.* **45**, 206-224 (2006).

52 Bloom, A. J., Smart, D. R., Nguyen, D. T. & Searles, P. S. Nitrogen assimilation and growth of wheat under elevated carbon dioxide. *Proc. Natl. Acad. Sci. U. S. A.* **99**, 1730-1735 (2002).

53 Rachmilevitch, S., Cousins, A. B. & Bloom, A. J. Nitrate assimilation in plant shoots depends on photorespiration. *Proc. Natl. Acad. Sci. U. S. A.* **101**, 11506-11510 (2004).

54 Loladze, I. Hidden shift of the ionome of plants exposed to elevated CO_2 depletes minerals at the base of human nutrition. *eLife* **3**, doi:10.7554/eLife.02245 (2014).

55 Montes-Bayón, M., Blanco-González, E. & Michalke, B. in *Metallomics* (ed Bernhard Michalke) Ch. 12, 339-357 (Wiley-VCH Verlag GmbH & Co. KGaA, 2016).

56 Foster, A. W., Osman, D. & Robinson, N. J. Metal Preferences and Metallation. *J. Biol. Chem.* **289**, 28095-28103, doi:10.1074/jbc.R114.588145 (2014).

57 Dudev, T. & Lim, C. Competition among metal ions for protein binding sites: determinants of metal ion selectivity in proteins. *Chemical reviews* **114**, 538-556 (2013).

58 Roberts, B. R. *et al.* Metalloproteomics: Principles, challenges and applications to neurodegeneration. *Frontiers in Aging Neuroscience* **5**, doi:10.3389/fnagi.2013.00035 (2013).

59 Bock, C. W., Katz, A. K., Markham, G. D. & Glusker, J. P. Manganese as a replacement for magnesium and zinc: functional comparison of the divalent ions. *Journal of the American Chemical Society* **121**, 7360-7372 (1999).

60 Andrews, T. J. & Kane, H. J. Pyruvate is a by-product of catalysis by ribulosebisphosphate carboxylase/oxygenase. *J. Biol. Chem.* **266**, 9447-9452 (1991).

61 Brown, D. A. & Cook, R. A. Role of metal cofactors in enzyme regulation. Differences in the regulatory properties of the *Escherichia coli* nicotinamide adenine dinucleotide phosphate-specific malic enzyme, depending on whether magnesium ion or manganese (2+) ion serves as divalent cation. *Biochemistry* **20**, 2503-2512 (1981).

62 Artus, N. & Edwards, G. NAD-malic enzyme from plants. *FEBS Lett.* **182**, 225-233 (1985).

63 Chang, G.-G. & Tong, L. Structure and function of malic enzymes, a new class of oxidative decarboxylases. *Biochemistry* **42**, 12721-12733 (2003).

64 Wheeler, M. C. G. *et al. Arabidopsis thaliana* NADP-malic enzyme isoforms: high degree of identity but clearly distinct properties. *Plant Mol.Biol.* **67**, 231-242 (2008).

65 Müller, G. L., Drincovich, M. F., Andreo, C. S. & Lara, M. V. *Nicotiana tabacum* NADP-malic enzyme: cloning, characterization and analysis of biological role. *Plant and cell physiology* **49**, 469-480 (2008).

66 Bloom, A. J., Burger, M., Asensio, J. S. R. & Cousins, A. B. Carbon dioxide enrichment inhibits nitrate assimilation in wheat and *Arabidopsis*. *Science* **328**, 899-903, doi:10.1126/science.1186440 (2010).

67 Husic, H. D. & Tolbert, N. Anion and divalent cation activation of phosphoglycolate phosphatase from leaves. *Arch. Biochem. Biophys.* **229**, 64-72 (1984).

68 Kim, Y. *et al.* Structure-and function-based characterization of a new phosphoglycolate phosphatase from Thermoplasma acidophilum. *J. Biol. Chem.* **279**, 517-526 (2004).

69 Dukes, J. S. *et al.* Responses of grassland production to single and multiple global environmental changes. *PLos Biol.* **3**, 1829-1837 (2005).

70 Rasse, D. P., Peresta, G. & Drake, B. G. Seventeen years of elevated CO_2 exposure in a Chesapeake Bay Wetland: sustained but contrasting responses of plant growth and CO_2 uptake. *Global Change Biol.* **11**, 369-377 (2005).

71 Korner, C. Plant CO_2 responses: an issue of definition, time and resource supply. *New Phytol.* **172**, 393-411 (2006).

72 Kimball, B. A., Idso, S. B., Johnson, S. & Rillig, M. C. Seventeen years of carbon dioxide enrichment of sour orange trees: final results. *Global Change Biol.* **13**, 2171-2183 (2007).

73 Norby, R. J., Warren, J. M., Iversen, C. M., Medlyn, B. E. & McMurtrie, R. E. CO_2 enhancement of forest productivity constrained by limited nitrogen availability. *Proc. Natl. Acad. Sci. U. S. A.* **107**, 19368-19373, doi:10.1073/pnas.1006463107 (2010).

74 Talhelm, A. F. *et al.* Elevated carbon dioxide and ozone alter productivity and ecosystem carbon content in northern temperate forests. *Global Change Biol.* **20**, 2492-2504, doi:10.1111/gcb.12564 (2014).

75 Myers, S. S. *et al.* Increasing CO_2 threatens human nutrition. *Nature* **510**, 139-142, doi:10.1038/nature13179 (2014).

76 Ehleringer, J. R., Cerling, T. E. & Helliker, B. R. C_4 photosynthesis, atmospheric CO_2, and climate. *Oecologia* **112**, 285-299 (1997).

77 Collatz, G. J., Berry, J. A. & Clark, J. S. Effects of climate and atmospheric CO_2 partial pressure on the global distribution of C_4 grasses: present, past, and future. *Oecologia* **114**, 441-454, doi:10.1007/s004420050468 (1998).

78 Skillman, J. B. Quantum yield variation across the three pathways of photosynthesis: not yet out of the dark. *J. Exp. Bot.* **59**, 1647-1661, doi:Doi 10.1093/Jxb/Ern029 (2008).

79 Galmés, J. *et al.* Expanding knowledge of the Rubisco kinetics variability in plant species: environmental and evolutionary trends. *Plant Cell Environ.* **37**, 1989-2001, doi:10.1111/pce.12335 (2014).

80 Tcherkez, G. G. B., Farquhar, G. D. & Andrews, T. J. Despite slow catalysis and confused substrate specificity, all ribulose bisphosphate carboxylases may be nearly perfectly optimized. *Proc. Natl. Acad. Sci. U. S. A.* **103**, 7246-7251 (2006).

81 Busch, F. A., Sage, R. F. & Farquhar, G. D. Plants increase CO_2 uptake by assimilating nitrogen via the photorespiratory pathway. *Nature Plants* **4**, 46-54, doi:10.1038/s41477-017-0065-x (2018).

82 Silva-Pérez, V., Furbank, R. T., Condon, A. G. & Evans, J. R. Biochemical model of C_3 photosynthesis applied to wheat at different temperatures. *Plant Cell Environ.* **40**, 1552-1564 (2017).

83 Walker, B. J. *et al.* Uncertainty in measurements of the photorespiratory CO_2 compensation point and its impact on models of leaf photosynthesis. *Photosynth. Res.* **132**, 245-255 (2017).

84 Luomala, E., Laitinen, K., Sutinen, S., Kellomäki, S. & Vapaavuori, E. Stomatal density, anatomy and nutrient concentrations of Scots pine needles are affected by elevated CO_2 and temperature. *Plant Cell Environ.* **28**, 733-749 (2005).

85 Hermida-Carrera, C., Kapralov, M. V. & Galmés, J. Rubisco catalytic properties and temperature response in crops. *Plant Physiol.* **171**, 2549-2561, doi:https://doi.org/10.1104/pp.16.01846 (2016).

86 Bauwe, H. in *C_4 Photosynthesis and Related CO_2 Concentrating Mechanisms* (eds Agepati S. Raghavendra & Rowan F. Sage) 81-108 (Springer, 2010).

87 Khoshravesh, R. *et al.* C_3–C_4 intermediacy in grasses: organelle enrichment and distribution, glycine decarboxylase expression, and the rise of C_2 photosynthesis. *J. Exp. Bot.* **67**, 3065-3078 (2016).

88 Creutz, C. & Sutin, N. Reaction of tris (bipyridine) ruthenium (III) with hydroxide and its application in a solar energy storage system. *Proc. Nat. Acad. Sci. USA* **72**, 2858-2862 (1975).

89 Bock, C. *et al.* Estimation of excited-state redox potentials by electron-transfer quenching. Application of electron-transfer theory to excited-state redox processes. *Journal of the American Chemical Society* **101**, 4815-4824 (1979).

90 Sattler, W. *et al.* Generation of powerful tungsten reductants by visible light excitation. *Journal of the American Chemical Society* **135**, 10614-10617 (2013).